International Journal of Applied Earth Observation and Geoinformation 122 (2023) 103400

Contents lists available at ScienceDirect

International Journal of Applied Earth Observation and Geoinformation

journal homepage: www.elsevier.com/locate/jag

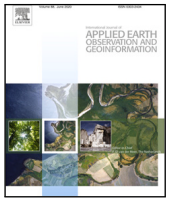

Automating the inventory of the navigable space for pedestrians on historical sites: Towards accurate path planning

D. Treccani [a,*], A. Fernández [b], L. Díaz-Vilariño [b], A. Adami [a]

[a] Department of Architecture, Built Environment and Construction Engineering. Politecnico di Milano, UNESCO Research Lab, Mantua Campus, Piazza C. d'Arco, 3, Mantova, 46100, Italy

[b] CINTECX, Universidade de Vigo, GeoTECH group, Vigo, 36310, Spain

ARTICLE INFO

Keywords:
LiDAR
Pavement inventory
Material inventory
Point cloud processing
Accessibility
Cultural heritage

ABSTRACT

Pedestrian mobility networks have a primary role on historical urban areas, hence knowledge of navigable space for pedestrians becomes crucial. Collection and inventory of those areas can be conducted by exploiting several techniques, including the analysis of point clouds. Existing point cloud processing techniques are typically developed for modern urban areas, which have standard layouts, and may fail when dealing with historical sites. We present a complete and automated novel method to tackle the analysis of pedestrian mobility in historic urban areas. Starting from a mobile lasers canning point cloud, the method exploits artificial intelligence to identify sidewalks and to characterize them in terms of paving material and geometric attributes. Output data are vectorized and stored in a very accurate high-definition shapefile representing the sidewalk network. It is used to automatically generate pedestrian routes. The method is tested in Sabbioneta, an Italian historic city. Paving material segmentation showed accuracy of 99.08%; urban element segmentation showed an accuracy of 88.2%; automatic data vectorization required only 1.3% of manual refinement on the generated data. Future advancements of this research will focus on testing the method on similar historical cities, using different survey techniques, and exploiting other possible uses of the generated shapefile.

1. Introduction

European Commission defines smart cities as *places where traditional networks and services are made more efficient with the use of digital solutions for the benefit of its inhabitants and business* (European Commission, 2023). Furthermore, the importance of digital solutions for better management of the city and its mobility network is enhanced. In recent years there has been a strong push towards development and implementation of smart city concept (Kim, 2022), both at decision-making and scientific levels. Within the various scientific fields concerned with the topic, it is remarkable the synergy between Geomatics, Information and Communication Technologies, and city planning (Mortaheb and Jankowski, 2022; Heidari et al., 2022).

Mobility management, intended as the ability to move freely and easily between two points of the city, can be identified as one of the most interesting aspects of this emerging paradigm. In this context, the term smart mobility is often used to highlight its importance for the development of a smart city (Šurdonja et al., 2020). To foster smart mobility in urban areas, it becomes essential to ensure an efficient transportation network, which must comprehend private vehicular traffic, public transportation and pedestrian mobility. Focusing then on pedestrians, the proper management and maintenance of sidewalks, pedestrian areas, arcades, squares and their connections have great importance. Plus, in order to ensure physical accessibility to places, specific actions that take into consideration several issues of the public space (Marconcini, 2018) should be considered. One of them is to grasp the knowledge of the characteristics of the connection ways (e.g., sidewalks), and their correspondence with national standards concerning physical accessibility.

Within this context, it becomes essential to develop solutions that enable rapid and effective data collection. In particular, an up-to-date inventory of relevant information on the networks that enable urban pedestrian mobility is of essential importance for all future planning, maintenance, and broader management actions on the urban structure. An excellent example of data collection is crowdsourcing, which is used in the case of project sidewalk (Saha et al., 2019) and wheelmap (Mobasheri et al., 2017). Both rely on data provided by users who voluntarily contribute to replenishing project databases. Another data collection method is the performance of manual in-situ measurements by specialized technicians. Other methods, instead, involve the

* Corresponding author.
E-mail addresses: daniele.treccani@polimi.it (D. Treccani), antfdez@uvigo.gal (A. Fernández), lucia@uvigo.gal (L. Díaz-Vilariño), andrea.adami@polimi.it (A. Adami).

https://doi.org/10.1016/j.jag.2023.103400
Received 5 April 2023; Received in revised form 29 May 2023; Accepted 21 June 2023
Available online 8 July 2023

use of artificial intelligence techniques aimed at analysing geospatial data (Hou and Ai, 2020). The data collected are then generally used to create maps for decision-making and as support for route design and scheduling of maintenance and interventions. This article is focused on the analysis of geospatial data exploiting artificial intelligence and automatized techniques focusing on pedestrian mobility networks and city's sidewalks.

In scientific literature, there are various articles dealing with automatic sidewalk recognition and assessment through point cloud analysis (Ai and Tsai, 2016; Hou and Ai, 2020; Halabya and El-Rayes, 2020). In those cases, the methods are based on modern and standardized urban infrastructure patterns. For example, a curb separating the street from the sidewalk and a different elevation of the two elements are often considered prerequisites.

This paper presents a complete and automated method for the characterization of urban navigable areas for pedestrians on historic sites, analysing and processing a point cloud. A historic urban area has elements of peculiarity in which it is not always possible to identify standard layouts. Existing methods to locate and assess sidewalks are based on standard urban areas and are prone to fail when used in historic cities.

Historic urban layouts rarely follow standardized logic but are often a set of ad hoc solutions that actually make the historic urban environment unique. Such solutions are commonly the result of successive interventions over time, that attempt to blend well with the historic urban tissue of which they are part. By carefully observing various historic cities and historic districts of various towns, we noticed one frequent peculiarity: roadways and sidewalks are at the same elevation and are not separated by curbs. Instead, they can be identified because they are paved with different materials.

Therefore, the procedures of this paper exploit differences in urban pavings. The difference in pavings is exploited by Machine Learning (ML) and Deep Learning (DL) approaches to segment sidewalks on the point cloud and identify their paving material.

The novel method we propose here is improved and extended with respect to some preliminary results previously communicated and focused only on some steps. Here we describe a complete workflow that from a given raw data input (point cloud) allows obtaining a very accurate vector file containing a correctly spatially referenced network of the navigable space for pedestrians in historical sites. Based on that network, routing analyses are then carried out. The method is developed entirely with *Python*, using specific libraries for point cloud management, ML, and DL workflows. The resulting vector file is then published on *GitHub*, and used for updating OpenStreetMap (OSM) dataset of the city selected as case study: Sabbioneta, a historic city and UNESCO site located in northern Italy.

The article is organized as follows. Section 2 presents articles related to point cloud processing for urban accessibility management and sidewalk inventory. Section 3 widely describes the method, focusing on and describing in detail each step. Section 4 presents the case study identified for the test phase, results and discussion. Section 5 is devoted to conclusions and future works.

2. Related work

The use of point cloud processing methods for the management of pedestrian mobility in urban areas is a well-investigated topic in scientific literature. The role of point clouds is manyfold: they could be segmented and analysed in order to search and inventory specific elements of the urban scene; they could be used as support for the generation of navigable routes within the city; and they could be a way to assist the physical accessibility assessment of the city.

Regarding the detection of urban objects, there is a great interest in curb identification, because they are the element of separation between roadway and sidewalk. For example, Serna and Marcotegui (2013) focused on the detection of curbs on Mobile Laser Scanning (MLS) point cloud. They segmented urban objects using range images as well as height and geodesic features. They performed accessibility analysis using geometrical features and accessibility standards. Then, they built an obstacle map for the generation of adaptive itineraries considering wheelchair users. curb detection and classification were also performed by Ishikawa et al. (2018), who extracted curbs from MLS and then classified them into two categories: those that allow access to off-road facilities and those that do not. By categorizing the curb types they assessed also the accessibility. The method was based on analysis of the angles of adjacent points on a scan line, then a voting process was implemented using surrounding classification results. A method to automatically classify urban ground elements from MLS data was also proposed by Balado et al. (2018). Their method was based on a combination of topological and geometrical analysis. Element classification was based on adjacency analysis and graph comparison. *Road*, *tread*, *riser*, *curb* and *sidewalk* were detected to provide valuable data from an accessibility point of view.

Regarding sidewalk inventory and assessment, Ai and Tsai (2016) extracted sidewalks and curb ramps from a combination of images and mobile LiDAR, based on some specific dimensional characteristics of curbs. The sidewalk features (width and slope) were measured and compared with the American with Disabilities Act (ADA), and the resulting data were stored in a GIS layer. Similarly, Hou and Ai (2020) proposed a deep neural network approach to extract and characterize sidewalks from LiDAR data. The stripe-based sidewalk extraction was also able to detect sidewalks' geometry features like width, grade, and cross slope, and compare them with ADA requirements. To support administrations in assessing existing conditions of sidewalk networks and their compliance with accessibility requirements, Halabya and El-Rayes (2020) used ML, photogrammetry and point cloud processing to extract sidewalk dimensions and conditions. Further approaches to sidewalk detection refer first to road boundaries detection and then to curb detection methods to separate road pavement from roadside (Ma et al., 2018). Regarding sidewalk materials, Hosseini et al. (2022a) proposed a method to classify sidewalk materials on photos, based on a DL technique and capable of recognizing several urban fabrics.

The topic of computation of navigable routes in outdoor environments typically includes a first part concerning the classification of urban elements and their accessibility evaluation, followed by the calculation of routes through a pathfinding algorithm. An example of this approach has been presented by López-Pazos et al. (2017) and Balado et al. (2019), who proposed a method for the direct use of MLS point clouds for the generation of paths for pedestrians with different motor skills and also considering possible barriers for people with reduced mobility. The method involved using an already classified point cloud, obstacle refinement, graph modelling and the creation of paths. Similarly, the project presented by Arenas et al. (2016) and by Corso Sarmiento and Casals Fernández (2017), had the main goal of developing a tool to assess the accessibility of public space and compute optimal routes. The tool was developed both on web and mobile phone platforms. The starting point of the work was TLS point clouds analysed through specific algorithms. The results were stored in specific GIS raster layers and applied for further accessibility studies. Another example, proposed by Luaces et al. (2021), aimed at computing accessible routes integrating data from multiple sources. In this work, the starting dataset was OSM, which was improved with information extracted from MLS point clouds (*ramps*, *steps*, *pedestrian crossings*). Obstacles and accessibility problems were detected by analysing social network interactions. The computed routes were generated by considering all the needs and limited mobility of each individual and were provided to final users employing a specifically developed mobile application. Another comprehensive work was proposed by Ning et al. (2022), which converted street view images into land cover maps, identified sidewalks, computed their widths and generated a sidewalk network. Similarly, Hosseini et al. (2022b) developed a sidewalk network dataset based on ML and computer vision techniques applied to aerial images.

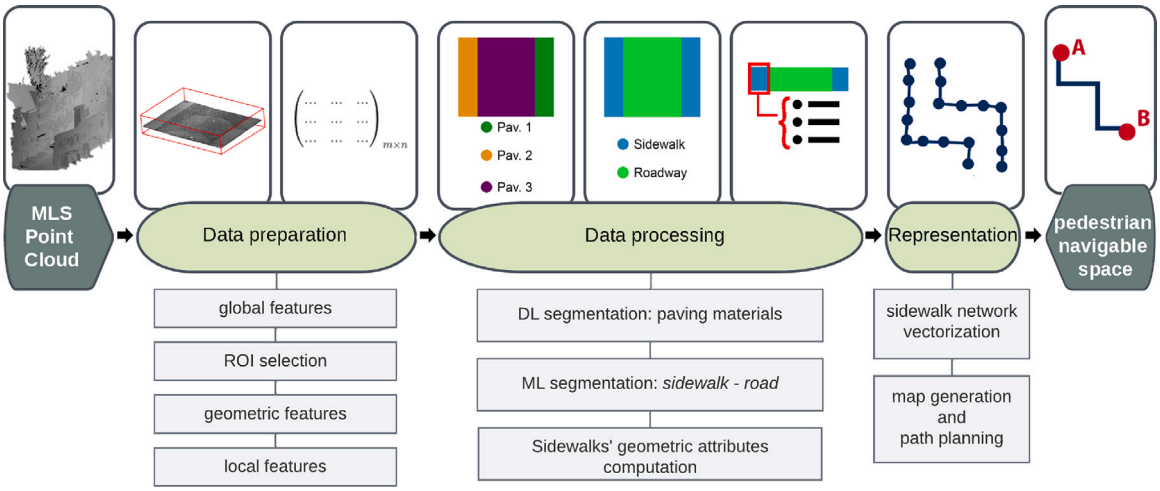

Fig. 1. Conceptual scheme of the workflow presented in this paper. The method takes as input data a point cloud of an urban environment, it performs automatic computations focusing on the sidewalks of the city. The workflow includes data preparation, data processing through ML and DL, sidewalks' attribute computation, and vectorization of the extracted information. The output data is a representation of pedestrian navigable space which contains also sidewalks specific information.

In contrast to previously described works, in this paper, the urban area investigated is a historic city. Urban object segmentation cannot be based on curb detection, and the peculiarity of urban element organization should be taken into consideration. In light of that, a novel automatic procedure is presented that allows the generation of an accurate and realistic vector network representing the sidewalks of the historic city including some of their geometric attributes and their pavings information.

The topic of accessibility management in historic urban environments through the use of point clouds has been covered by a doctoral thesis (Treccani, 2022), from which the idea of the method presented in this paper is derived. Compared with the aforementioned thesis, the method discussed here is more comprehensive and sophisticated.

Concretely, the improvement over the previous work is threefold:

- This paper presents the refined and strengthened version of the general workflow, which was never published as a whole, and where each step is carefully developed and commented on. Previously published results described only some steps of the general workflow and were tested on smaller areas.
- Here, the semantic segmentation of the point cloud into *sidewalk* and *road* exploits ML approach, through a Random Forest (RF) classifier, showing higher performances with respect to previous work.
- Here, paving material segmentation is based on a DL approach applied on the rasterized point cloud, performing a reprojection of predicted values onto the points of the point cloud.

3. Materials and method

The methodology (Fig. 1) is composed of three main steps: preparation of the raw data, data processing, and representation of the data for pedestrian mobility purposes.

The pre-processing step consists of the subdivision into Regions of Interest (ROIs), and the computation of several features on the point clouds. The processing phase includes a DL segmentation, applied on raster images generated from the ROIs point clouds. The predicted values, related to paving materials composing the ground surfaces, are re-projected back onto the points. Then, following a ML approach, the ROIs are segmented into *road* and *sidewalk*. The cluster of points labelled as *sidewalk* are then used to compute some sidewalk's geometric attributes. The representation of the data involves the vectorization of the sidewalks network and the computed attributes. The output data are used for the generation of accurate pedestrian mobility paths, taking into account physical accessibility needs and National regulations.

Table 1
Point features computed and used in the workflow. Global features are computed on the whole point cloud, local features and geometric features are computed after the subdivision of the point cloud into ROIs.

Features	Values
Global features	Intensity, RGB, HSV
Geometric features	Roughness, Omnivariance, Sphericity, Anisotropy, Normal change rate, Verticality, Normal vector
Local features	Relative elevation, Relative distance

3.1. Data preparation

The input data is a MLS point cloud of a historic urban environment, correctly georeferenced and provided with trajectory data. The point cloud is here subdivided in ROIs and point features are computed, recalled by Table 1.

3.1.1. Global features

Some point attributes, acquired by the survey instrument, are automatically stored within the MLS point cloud. The ones used in this work are the Intensity and the Red Green Blue (RGB) colour data for each point. The Intensity is a function of several variables, including the distance from the laser, the angle of incidence of the laser beam on the surface and the specific material reflectance (Yuan et al., 2020), and can be intended as the amount of energy of the backscattering signal of the instrument. RGB data are acquired using cameras equipped on the MLS system. The colour space is then changed from RGB to Hue Saturation Value (HSV). By doing so, brightness data are stored within the V channel and the influence of shadows and sunny areas can be controlled (Pierdicca et al., 2020).

3.1.2. Selection of the region of interest

The point cloud is subdivided into several ROIs along the MLS trajectory. The purpose is twofold: the reduction of memory consumption during computation, and the focus of the analysis by discretizing the road environment into portions of fixed extension along the road trajectory. By doing so, we can control the resolution of the output data. In fact, since the final output data is a sidewalk network whose edges and attributes are computed on the basis of the ROIs, its resolution is proportional to the dimension of the ROI itself.

ROIs are generated by cropping the point cloud following the survey trajectory (i.e., along the road route), using a set of oriented Bounding Boxes (BBs). The BB orientation is based on two consecutive points at

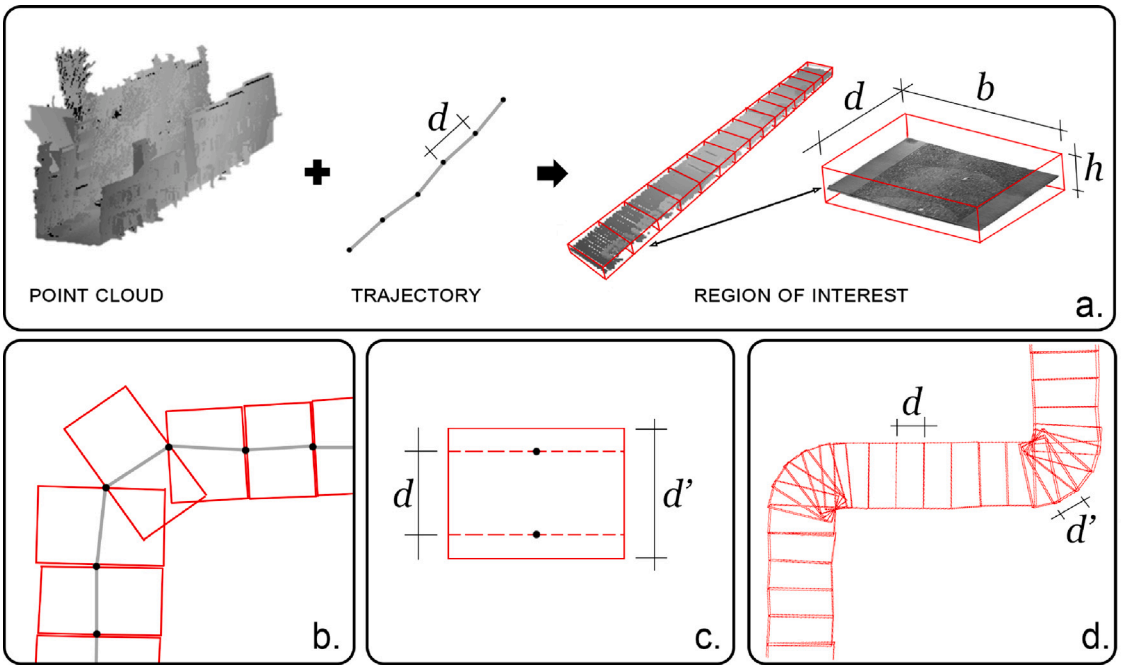

Fig. 2. Regions of Interest (ROI) generation detailed schemes. (a) Diagram of the subdivision of the initial point cloud into several ROIs using the trajectory data and a set of Bounding Boxes of dimensions *d*, *b*, *h*. (b) Example of ROI selection in a corner; it is noticeable how some portions of the point cloud can be not selected, in particular in the corner position. (c) Increase of ROI length for corner areas, from length d to d'. (d) Example of Bounding Boxes width d for straight portions of road and d' for bends, to ensure that all points are selected also in bends.

a fixed d distance extracted along the trajectory line (Fig. 2a). The Z coordinate of trajectory points corresponds to the instrument position (on top of the car). For the purpose of the BB creation, those points are projected on the ground surface of the road by moving their Z value. The main BB dimension is the d distance, the other two dimensions are a width b selected bigger than the average road width, and a height h centred on the road level and selected bigger enough to ensure the selection of points on the ground surface (Fig. 2a).

Typically in historical cities, straight portions of roads are not so long, while sharp bends and crossings with other roads are very common. In those areas, the oriented BB could not be able to include all the necessary points, as in the example provided by Fig. 2b. To cope with that, BBs in those areas are enlarged and their length is increased to d' (Fig. 2c and d). Plus, an overlap between neighbouring BBs is implemented in those specific areas. The value of d' is selected after several empirical tests, looking at the coverage of the ROIs on the point cloud in road bend areas. The value of d' is defined such that $d' = 1.5d$ and so it is directly related to the chosen value of d.

Following this iterative process, starting from the first point of the trajectory and moving, two by two, to the last point, the point cloud is subdivided into ROIs. Then, on each ROI a refinement of the selection is implemented to remove points not pertaining to ground surfaces. Firstly, the exclusion of points inside buildings, exploiting the OSM building footprint dataset. Secondly, the removal of points aligned on vertical surfaces, exploiting the N_z component of the Normal vector of each point.

During the survey of the city, it may happen that the LiDAR mounted on the instrument acquires also some points of objects inside the houses, passing through windows. To remove those points and other possible noisy points the OSM dataset can be used. OSM dataset can be downloaded for free from the website or using specific plugins existing for commercial or open-source GIS software. All the layers containing *building* as Key value are downloaded and used to define polygons representing the buildings' footprint of the city. All points of the ROI within these polygons are then removed from the ROI (Fig. 3).

Lastly, all the points aligned on the façades of the buildings or on other vertical surfaces are selected by relying on the Z component (N_z) of the normal vector of each point and are removed. In order to do that, all points with a value of N_z lower than a specific threshold $N_{z,lim}$ are considered points aligned on vertical surfaces, and removed. The value of $N_{z,lim}$ is established after empirical investigation.

3.1.3. Geometric features

Geometric features are derived from the covariance matrix of the 3D structure tensor computed on the point neighbourhood (Weinmann et al., 2017, 2015). They describe the arrangement in space of points within the considered neighbourhood. Geometric features are here computed using the open-source software CloudCompare (www.cloudcompare.org). The software allows to compute several geometric features; within the workflow, only some features are selected and effectively used (reported by Table 1). Additionally, also the Normal vectors of points are computed.

3.1.4. Local features

These features, which we define as local features, are computed on each ROI, rely on the relation of each point to the surrounding environment, and are specifically focused on the road and sidewalk areas. These features are the relative elevation Z_{rel} and the relative distance d_{rel}, calculated as a function of the centre line of the road derived from the trajectory. The two features are computed as relative and not absolute values so that they determine the relative position of each point in a generic cross-section of the road. In that way, points on different road widths maintain the same proportion and are comparable.

The relative elevation Z_{rel,P_2} of the generic point P_2 is computed as the difference between the elevation Z_{P_2} of the point P_2 (Fig. 4b), and the average elevation $Z_{centreline}$ of the centreline of the road, as in the following:

$$Z_{rel,P_2} = \left| Z_{P_2} - Z_{centreline} \right| \tag{1}$$

where the elevation of the centreline ($Z_{centreline}$) is computed as the average value of Z coordinate of points on the trajectory falling within the ROI. This feature is helpful for the exceptional areas where sidewalks have higher elevations with respect to the roadway.

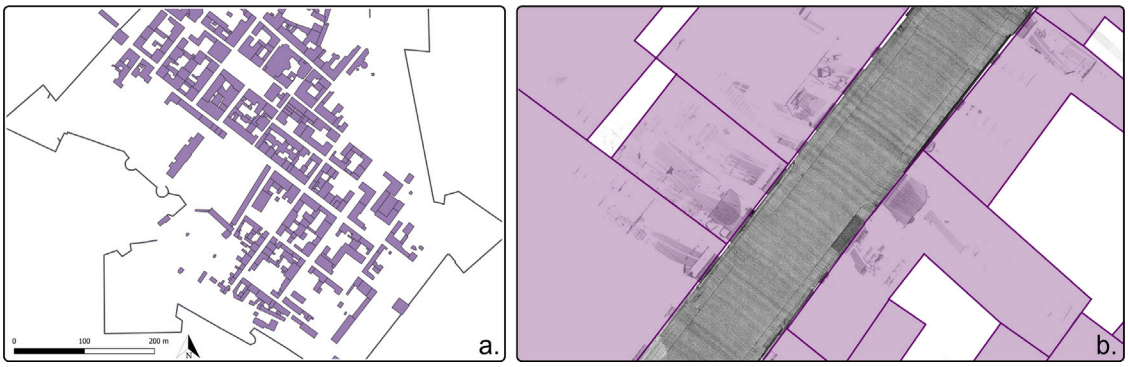

Fig. 3. OpenStreetMap dataset is used to remove noisy points not related to the road environment. (a) *building* dataset downloaded from OSM for the case study presented in this paper, all visible polygons represent the building footprint. (b) example of a road point cloud with noisy points inside buildings (e.g., scanned elements by laser passing through windows or open doors). In the method, the noisy points are selected when they are inside the building footprint and then removed.

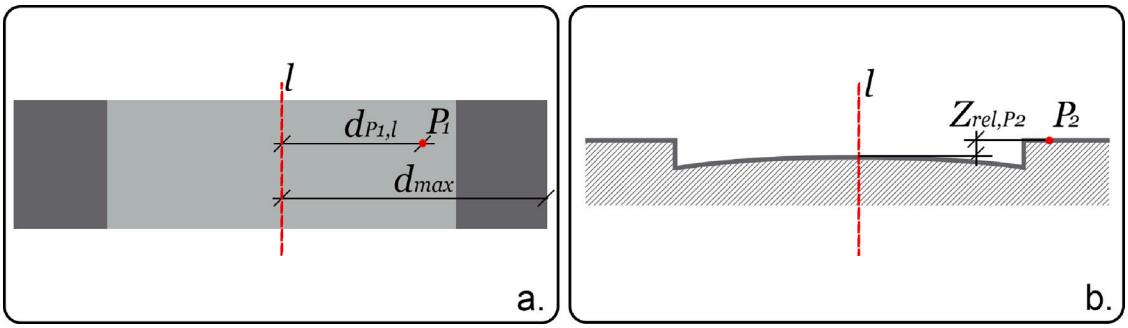

Fig. 4. Scheme of local features calculation. (a) The relative distance d_{rel} of a generic point P_1 is defined as the euclidean shorter distance $d_{P_1,l}$ from point P_1 to the line l, divided by the maximum distance d_{max}. (b) The relative elevation Z_{rel,P_2} of the generic point P_2 is computed as the difference between the elevation Z_{P_2} of the point P_2 and the average elevation $Z_{centreline}$ of the road's centreline.

The relative distance d_{rel,P_1} of a generic point P_1 is computed by relying on the trajectory from the instrument, which is assumed to correspond to the road centreline. For each ROI the trajectory is considered as a single straight line of equation $l : ax + by + c = 0$, where a, b, c are the coefficient of the straight line general equation. Then, the relative distance d_{rel,P_1} of the generic point $P_1 : (x_{P_1}, y_{P_1})$ (Fig. 4a) is computed by the euclidean shorter distance $d_{P_1,l}$ from point P_1 to the line l, divided by the maximum distance d_{max} identified within the same ROI. The relative distance can be computed as:

$$d_{rel,P_1} = \frac{d_{P_1,l}}{d_{max}} \tag{2}$$

where:

$$d_{P_1,l} = \frac{\left|ax_{P_1} + by_{P_1} + c\right|}{\sqrt{a^2 + b^2}} \tag{3}$$

An exception is defined for relative distance computation in ROI including road crossings. In those cases, unlike in straight road portions, the trajectory line might be inclined and not parallel to sidewalks, and it could not be useful to compute the road proportions. To cope with that, OSM dataset is exploited. In OSM roads are represented by polylines, and can be downloaded using the key *roadway*. These polylines are used as alternative trajectory lines for the representation of the road centreline. Plus, for those ROIs, the relative distance feature is computed differently. The modified relative distance $d'_{rel,P}$ of the generic point P (Fig. 5) in a ROI containing a crossing is computed as the geometric mean of the relative distances $d_{rel,P_{l_i}}$ between that point P and all the OSM lines l_i involved in the crossing, as follows:

$$d'_{rel,P} = \sqrt[n]{\prod_{i=1}^{n} d_{rel,P_{l_i}}} \tag{4}$$

where $d_{rel,P_{l_i}}$ are computed according to Eq. (2), and n is the maximum number of lines involved in the crossing (generally 2).

Fig. 5 shows two examples of crossings, where each point was coloured depending on the computed distance value in a colour scale that goes from blue for the lower values, passing to green and yellow, and with red for the higher values. It is clearly visible how d_{rel} mimics the proportion of the road.

3.2. Data processing

3.2.1. Paving materials segmentation

The goal of this phase is to identify the different paving materials on each ROI. The approach proposed here (Fig. 6) is based on Treccani et al. (2022a), which after rasterizing the point cloud, performed image segmentation using a Convolutional Neural Network (CNN). In this paper, a different neural network is used and the process is entirely developed in *Python*. Furthermore, the process is applied to the raster images generated from the ROIs, which after the segmentation, are reprojected back onto the ROIs, and stored as a point attribute. The reprojection method implemented is based on the one presented by Paz Mouriño et al. (2021), where the correspondence between ROI points and raster image pixel indexes is leveraged.

The ROI is rasterized by subdividing the XY plane into several cells, whose size is defined according to the raster resolution chosen. Each cell corresponds to a pixel in the rasterized image. The R, G, and B channels assigned to each pixel are here used to store not the point colour information, but three different point features. In fact, for the DL approach, R, G and B identify the input data that the network is fed with, so it is actually possible to convey within them other data than colour. The three selected features are Intensity, Roughness and Omnivariance. To complete the rasterization process, the RGB value

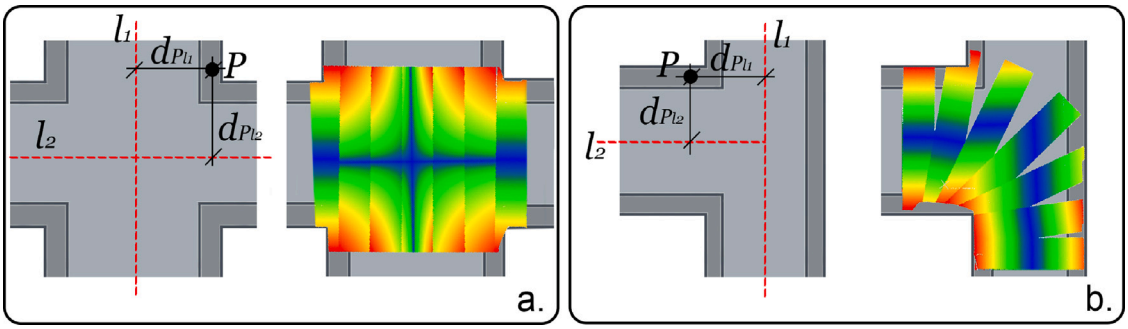

Fig. 5. Two examples of road crossings, where the relative distance is computed with a different approach (Eq. (4)). (a) A X-shaped crossing. (b) A T-shaped crossing. In both cases the image on the right shows several ROIs; each ROI is coloured depending on the computed relative distance d'_{rel} value in a colour scale that goes from blue for the lower values, passing to green and yellow, and with red for the higher values. It is clear how $d'_{rel,P}$ better describes the road shape. (For interpretation of the references to colour in this figure legend, the reader is referred to the web version of this article.)

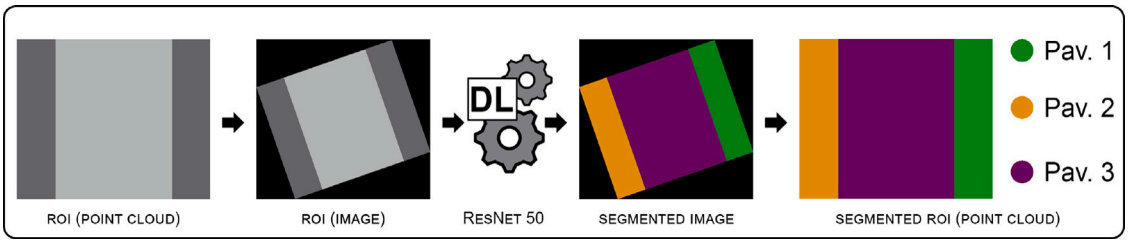

Fig. 6. Scheme of the DL classification. Each ROI is rasterized, the image is segmented using a DL approach (exploiting the model *Resnet 50*) into classes related to the paving materials present in the case study (*cobblestone*, *stone*, *brick*, *sampietrini*, *asphalt*), and the predicted attributes are projected back onto the points of the ROI.

of each pixel is then set as the average of the values of each specific feature of points falling inside the cell.

Since RGB channels have a strict range of values: $[0; 255]$, the features are normalized before applying the rasterization. The general formula used here for the normalization is $F_{norm} = (F - F_{norm})/(F_{max} - Fmin) * 255$, where F stands for a general feature. To define F_{min} and F_{max} different strategies are used, according to each feature's characteristics. Since the Intensity, in the case study dataset, is saved by the instrument processing software (from Leica) in a format with a defined range: $[-2048; 2048]$, this range limit is used to define the maximum and the minimum for the normalization. Specifically $I_{max} = 2048$ and $I_{min} = -2048$. Then, since the other two features do not have an absolute minimum or maximum value, F_{max} is defined as the maximum value of feature F over the considered dataset, and F_{min} the minimum value of feature F over the considered dataset.

The DL image segmentation is achieved by training a semantic segmentation neural net from *PyTorch* library, using the architecture *DeepLabv3*. The pre-trained model *Resnet50* is exploited, and Adam optimization algorithm is used. The training loop is developed using batches of 10 images in each iteration. The training dataset is selected from the areas of the city most representative of the paving materials. The reference values for the segmentation mask are taken from the Ground Truth (GT). The GT is manually created by expert architects, based on the paving materials actually present in the city. Classes for DL segmentation are identified depending on paving materials effectively present in the case study: *cobblestone*, *stone*, *brick*, *sampietrini*, *asphalt*. An additional class is used for the background pixels, named *background*. The resulting trained model is then applied to segment all the ROIs.

The process of reprojecting the classified images back to the point cloud take place by recalling the indexes of points falling within the XY cells (i.e. the image pixels). The classes predicted for each pixel are then conveyed to the corresponding points. As a result, points within the ROI have a new feature related to the paving material of the ground surface, this feature is used later within the methodology.

3.2.2. Ground elements segmentation

The purpose of this step is the segmentation of the urban ground surfaces of the city into *sidewalk* and *road*, and it is performed for each ROI. The segmentation is carried out using a ML approach, and a RF classifier is implemented from `scikit-learn` library. The RF classifier constructor provided by the library has several parameters, all of which are set to their default value. The classifier requires also to specify the Features to be used for the classification. They are selected by analysing the Feature Importance plot, which allows evaluation of the importance of each feature on the classification task. This plot is generated by using the `scikit-learn` library, and each bar of the plot shows the feature's importance. Fig. 7 shows a scheme of the ML approach.

The features included in the Feature Importance plot are the previously mentioned Local, Global, and Geometric features. Geometric features are computed with various neighbourhood *radii*, and among them the selected features are the ones with a higher rating in the Feature Importance plot, preferring those computed with a higher radius.

The RF classifier is trained and validated on a portion of the dataset. The training is based on the manually created GT. The two classes identified are *sidewalk* and *road*. The training dataset is selected including portions of the most representative road environments, considering all the possible scenarios that appear within the city. The trained model is then used to classify all the ROIs of the dataset. As a result, each point within each ROI is labelled according to the urban ground element.

3.2.3. Sidewalks' attributes computation

Focusing on the *sidewalk* class points of each ROI, some geometric attributes are computed and assigned to those points. The computed attributes are those deemed useful for technicians and professionals involved in the management, maintenance and design of the city's urban environment. For each sidewalk within the ROI, the computed attributes are width, transverse and longitudinal slopes, elevation with respect to the road surface, and main paving material. Some of them are estimated on the basis of some point attributes, and by applying

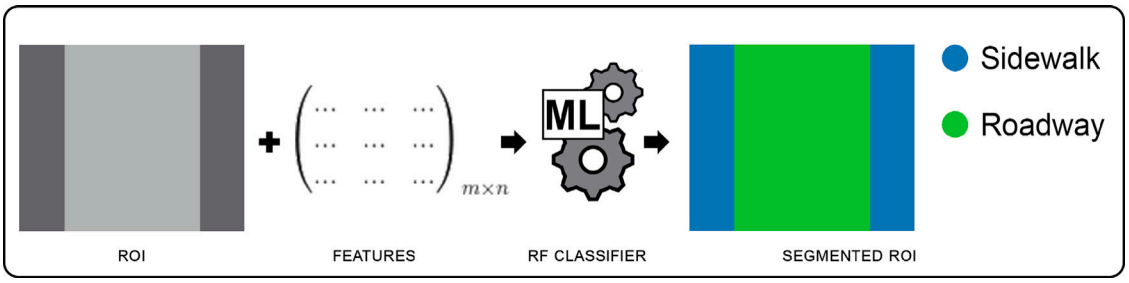

Fig. 7. Scheme of the ML segmentation. The points of each ROI are classified by a Random Forest classifier and two classes are predicted: *sidewalk* and *road*.

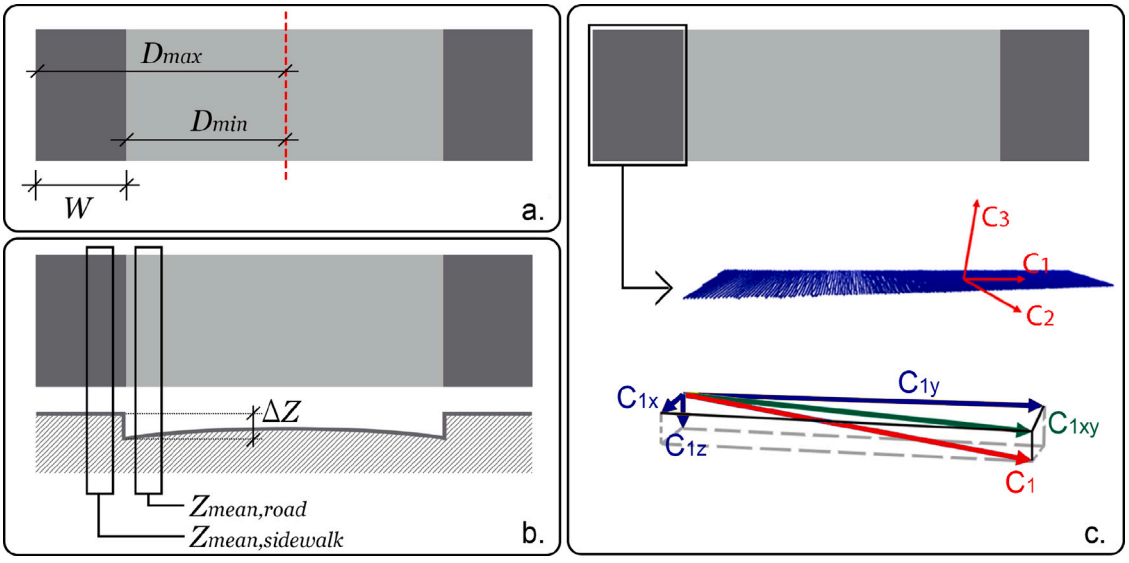

Fig. 8. Schemes showing the calculation of sidewalk attributes. (a) Average width W is computed as the difference between the distances of the closest (D_{min}) and the farthest (D_{max})points of the sidewalk cluster of points with respect to the road centreline. (b) The sidewalk relative elevation (ΔZ) is referred to the jump in elevation (if present) between the sidewalk ($Z_{mean,sidewalk}$) and the part of the road in close proximity to it ($Z_{mean,road}$). (c) Slope in the longitudinal and transverse directions ($Slope_{Long}$ $Slope_{Transv}$), computed by leveraging on the Principal Component Analysis, and exploiting the principal components C1 and C2.

specific formulas; others are derived simply by retrieving the value of features previously computed.

The methods used to calculate the attributes are listed below:

- The **average width** (W) is computed as the difference between the distances of the closest and the farthest points of the sidewalk cluster of points with respect to the road centreline. D_{min} is defined as the 5th percentile of all the distances in the ROI, and D_{max} is identified as the 95th percentile of all the distances. The approach is schematized by Fig. 8a, and the average width is computed as follows:

$$W = D_{max} - D_{min} \tag{5}$$

- The **sidewalk relative elevation** (ΔZ) is referred to the jump in elevation (if present) between the sidewalk and the part of the road in close proximity to it. Exploiting the distance feature, it is possible to select the band of points on the road that are on the boundary with the sidewalk and extract the mean value of their Z-coordinate. Similarly, a limited band of sidewalk points, adjacent to the boundary with the road points, is selected and the mean value of Z is extracted. Having defined the two reference height value ($Z_{mean,road}$ and $Z_{mean,sidewalk}$) (Fig. 8b), it is then possible to compute the height difference between the two urban elements as:

$$\Delta Z = \left| Z_{mean,sidewalk} - Z_{mean,road} \right| \tag{6}$$

- The **transverse and longitudinal slopes** ($Slope_{Long}$ $Slope_{Transv}$) are computed by leveraging on the Principal Component Analysis (PCA). Computing the PCA of XYZ attributes of a point cloud, the resulting eigenvectors can be used to describe the point cloud orientation. The three principal components are oriented in the three major directions that best fit and describe the point distribution in space. In the case of the sidewalk cluster of points, the three eigenvectors represent respectively the three main directions C_1, C_2, C_3 (Fig. 8c) on which points are distributed. The higher eigenvector is aligned longitudinally (C_1) on the cluster, the middle one is aligned transversely (C_2), and the smaller one is aligned in the normal direction (C_3). Considering then the vector oriented according to the longitudinal direction (C_1), by decomposing it on the three planes *xyz*, obtaining its three components, it is possible to compute the slope as referred to the angle between the vertical projection C_{1Z} and its *xy* projection $C_{1,XY}$:

$$Slope_{Long}\ [\%] = \frac{C_{1,Z}}{C_{1,XY}} = \frac{C_{1,Z}}{\sqrt{C_{1,X}^2 + C_{1,Y}^2}} * 100 \tag{7}$$

The same reasoning is then applied to eigenvector C_2 to compute the transversal slope. The equation is as follows:

$$Slope_{Transv}\ [\%] = \frac{C_{2,Z}}{C_{2,XY}} = \frac{C_{2,Z}}{\sqrt{C_{2,X}^2 + C_{2,Y}^2}} * 100 \tag{8}$$

- The **paving material** of the sidewalk is identified by defining the most frequent paving material attribute of the analysed cluster of points, as computed on Section 3.2.1.

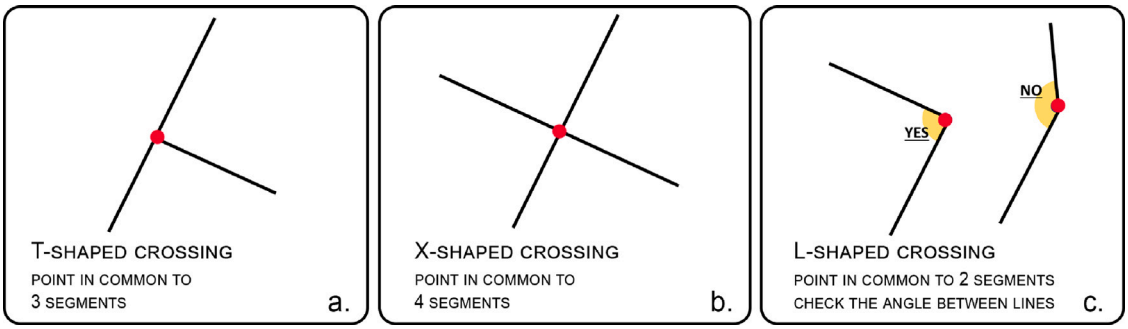

Fig. 9. Simplified diagram of the three crossing types identified and used within the workflow. OSM's dataset and reasoning about the multiplicity of points are exploited to identify the crossing type. (a) *T-shaped* crossing, when a point is in common to three lines. (b) *X-shaped* crossing, when the point is in common to two lines. (c) *L-shaped* crossing when a point is in common to two lines; in those cases, a check on the angle between lines is implemented; if the angle is in the range [80;100] degrees, the point is representative of an *L-shaped* crossing.

3.3. Representation

Several methods can be used for representing sidewalks and pedestrian mobility information collected from the point cloud. In scientific literature, some authors used directly the point cloud as a representation type for conveying and disseminating the data to final users, especially regarding 3D city modelling (Wegen et al., 2022; Nys et al., 2021). On the other hand, other authors performed path findings directly on the point cloud in urban environments (Balado et al., 2019).

In this paper, the representation type selected is a very accurate vector file for pedestrian mobility management. We believe that this type of representation is easier to be understood and used by a wider range of final users independently of their experience. This file is then used to compute pedestrian paths within the city, considering various sidewalks attributes and physical accessibility regulations as constraints.

3.3.1. Crossing identification

In order to correctly perform the vectorization of the sidewalk network, the knowledge of crossings position is fundamental. Three typologies of crossings between roads can be defined: we call it *T-shaped* crossing when one road enters another road making a *T* shape; we call it *X-shaped* crossing when two roads cross; and we define it as *L-shaped* crossing when two roads meet, creating an approximately 90-degree bend.

OSM dataset is used to identify road crossing position and type. In OSM roads are represented by polylines, and as different roads come together and create a crossroads in the city, in a similar way different polylines met at a single point on the dataset. Crossroads areas can be identified by exploiting points where polylines met. Then, to identify also the type of crossing, a simple reasoning is implemented (Fig. 9). The multiplicity of a point is used to identify the type of crossroads: if the point is in common with 3 lines it is a *T-shaped* crossing, if it is in common with 4 segments it is an *X-shaped* crossing, and if the multiplicity is 2, it could possibly be a *L-shaped* crossing, but in this last case a further check should be applied. In fact, a point in common to 2 lines could be every point of a polyline, made by several segments. To define if it is a *L-shaped* crossing the angle between the associated segments is checked. Since we define the *L-shaped* crossing as a bend of approximately 90 degrees, we choose that if the angle between the lines is in the range [80;100] degrees the point defines an *L-shaped* crossing, otherwise the point is not considered representative of a crossing.

3.3.2. Vectorization

The development of a Sidewalk network, composed of nodes and edges, follows a method previously presented (Treccani et al., 2022b). For each ROI, the centre of each *sidewalk* cluster of points is computed by averaging X and Y coordinates. The resulting point is converted into a node of the network. Then the nodes are joined by edges. Consecutive and neighbouring nodes are connected together, always comparing the location of the edges with the city's road network (derived from OSM), in order to avoid redundant edges or incorrect connections. This workflow is recalled by Fig. 10.

The topology of the Sidewalk network is ensured by the fact that the pattern and organization of urban elements (sidewalk and road, de facto) within the ROIs are uniform and consistent, and because consecutive ROIs were considered following the road path (i.e. the trajectory) and in continuity one with the other. The only discontinuity element are the crossings. Edges generation near crossings areas is done differently: a constraint is added that does not allow the creation of edges that cross the road (i.e., that intersect the polylines representing the centre of the road).

Crossings within the city are already identified and named as *L-*, *T-*, or *X- shaped*. Before performing the edges generation in crossing areas as previously described, node regularization in those areas is necessary. The correct identification of the type of intersections allows the computation of best-fitting lines and the regularization of the nodes' position by slightly adjusting their XY coordinates (Fig. 11). Lastly, a manual check is done to identify and correct any possible errors and to complete the network in any areas of the city that are not surveyed and of which data are missing.

During the development of the network, the attributes of the various portions of sidewalks are linked to the respective edge representing them. The output file of the workflow is a shapefile containing the sidewalk network filled with the attributes of the sidewalks themselves.

3.3.3. Routing analysis

The vector file is used to compute pedestrian paths within the city, taking into consideration accessibility regulations. There are a variety of software solutions, both commercial and open-source, that allow the calculation of pedestrian flow or that calculate routes. These analyses are here carried out using open-source software: QGIS (www.qgis.org).

Exploiting the *network analysis* tool on the processing toolbox of QGIS, the path between two points can be computed. This tool is capable of computing the shortest path between two selected points using as guidelines the edges of the previously computed sidewalk network.

Furthermore, instead of the shorter path, also the fastest path can be computed. This path is computed relying on a speed value given to each edge. By giving a fictitious speed value to the edges, proportional to the sidewalk accessibility attribute, it is possible to generate the most accessible path. A new attribute for the edges is created, representing the fictitious speed. This new attribute is based on the sidewalk geometric attribute and its comparison with National regulations about physical accessibility; a high speed is set for accessible edges and a low speed is set for non-accessible edges. The resulting path uses mostly the edges that are considered more accessible (i.e., the ones with higher speed).

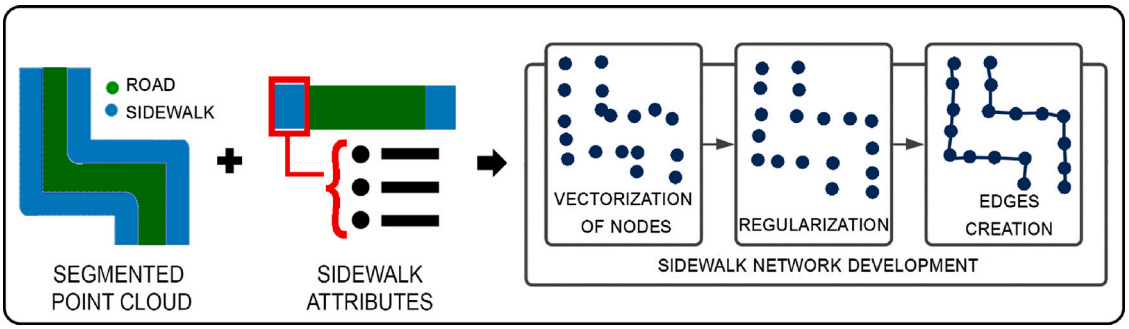

Fig. 10. Scheme of the process of data vectorization. The segmented ROIs (into *sidewalk* and *road*) and the sidewalks attributes (average width, relative elevation, longitudinal and transverse slopes, paving material) are used to generate the sidewalk network. The centre of each *sidewalk* points on the ROIs are transformed into nodes, which are regularized according to the road framework, and then connected by edges.

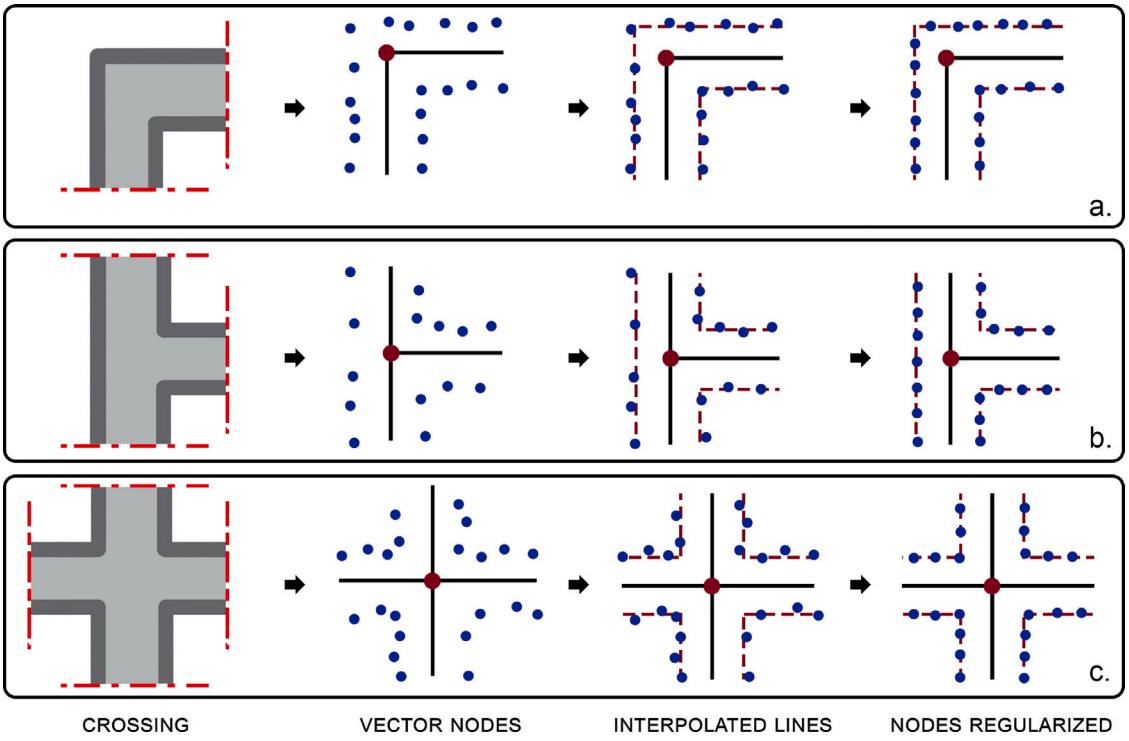

Fig. 11. Regularization of the network nodes for three types of crossing, named *L-shaped* (a), *T-shaped* (b), *X-shaped* (c). The process is the same for all crossings: first, nodes are vectorized, then lines are interpolated through nodes, taking into consideration the type of crossing and the road shape, and lastly, nodes are slightly moved to be on the best-fitted lines.

4. Results and discussion

4.1. Case study description

The case study selected is Sabbioneta, a historic city located in northern Italy. Sabbioneta was re-founded in the second half of the 16th century, based on a pre-existing medieval village. The city was built following the *ideal city* principles of the Italian Renaissance.

In 2008 Sabbioneta, together with the near city of Mantova, was inserted into the UNESCO World Heritage List. The two cities have been included in the list because they offer an exceptional testimony to the urban, architectural and artistic achievements of the Renaissance, linked together through the ideas and ambitions of the ruling family, the Gonzaga.

The historic city has a small areal extent, about 0.4 square kilometres. The street structure is organized into *cardi* and *decumani*, and it has a chessboard layout. The city consists of 34 blocks, fairly regular, rectangular or square in shape, but vary in size, with a predominantly east–west orientation (Lorenzi, 2020). The streets do not have a fixed width, varying from 5 m to 14 m wide stretches. Sometimes it happens that the change in width occurs within the same stretch of road, either slightly or more markedly. Remarking on this change in width, sometimes also the paving of the street roadway is different.

In Sabbioneta urban pavings assume the role of highlighting the destination of use of urban ground (Fig. 12). Roadways and sidewalks are often at the same elevation, but they can be identified because they are paved with different materials. Specifically, within the city, cobblestone, sampietrini and asphalt are typically used for the roadway surfaces, while bricks and stone (mainly porphyry) are used for the sidewalk surfaces. Table 2 describes the physical aspects of Sabbioneta pavings. The peculiar organization of the urban structure, and the stratification of various pavings within the city, make Sabbioneta a proper case study for testing the presented methodology.

Sabbioneta was surveyed with a MLS system: Leica Pegasus:Two, which mounted, as a laser scanner, a Z+F profile 9012. The profiler's main characteristics are recalled by Table 3. The instrument was mounted on top of a car, and almost the entire historic city was surveyed. The resulting point cloud covered almost 7 km of road and was

Fig. 12. Photos of the city of Sabbioneta, a case study for this paper. (a) Views of some streets in the city. (b) Layering of different pavements used for different elements of the urban area in the city, sidewalks and roads are highlighted by the use of different paving materials.

Table 2
Description of the 5 classes of paving materials identified in the case study, the city of Sabbioneta.

Paving material name	Description
Sampietrini	Squared stone blocks, aligned in consecutive radial grids (they can also be aligned on rectangular grids, but not in Sabbioneta). In Sabbioneta they are typically used for the road surface.
Bricks	Rectangular bricks arranged in a stretcher bond pattern. Typically in Sabbioneta, they are used for sidewalks, the largest dimension of the rectangle is orthogonal to the main direction of sidewalks.
Cobblestone	River stones lined up next to each other without any apparent regular arrangement. The individual elements are rounded and protrude from the surface. In Sabbioneta are typically used for roadway surface
Stone	Rectangular stone blocks, aligned on a regular grid similar to the English cross bond pattern. Typically used for sidewalks in Sabbioneta.
Asphalt	Homogeneous, mostly flat surface.

Table 3
Description of Z+F profile 9012 features, from technical data sheet. The profiler was mounted on the instrument used for data acquisition, Leica Pegasus:Two.

Feature	Value
Rotation speed	200 Hz
Coverage	one profile every 5 cm at a speed of 36 km/h
Acquisition range	from 0.3 to 119 m
Field of view	360°
Scan rate	1.016 million points per second
Accuracy	0.020 m RMS in horizontal and 0.015 m RMS in vertical

Table 4
Values of the pre-processing parameters used in the method.

Parameter	Value
d	2 m
d'	3 m
$N_{z,lim}$	0.8

composed of a total of 1.2 billion points. The instrument mounted 360-degree cameras, so the points attribute included the RGB colour. The dataset of Sabbioneta was organized by conducting several missions of acquisition while moving within the roads of the city (Fig. 13). The full-density point clouds (no subsampling of the data was done) of each mission together with the trajectory data are used.

For both the ML and DL approaches, one acquisition mission is identified as most representative of the city: Track C. This acquisition mission includes areas from outside the fortified walls, roads of various widths, and areas closer to squares and porticoes. This track also includes all paving materials identified within the city.

4.2. Results

4.2.1. Data preparation

For the definition of the BB size, after some empirical tests, the parameter d is set to 2 m, while d' for curved portions is set to 3 m. Then, for the refinement of the selection, the value of the limit parameter $N_{z,lim}$, is defined after empirical investigation. The $N_{z,lim}$ value is defined by making some tests setting it at different values and visually inspecting the point cloud to see which points were selected. For the point cloud of the case study a value of 0.8 was considered enough for the purposes. In fact, by setting it to 0.8, and then removing the points with $N_z < 0.8$, the resulting points belonged only to non-vertical surfaces, as desired. Table 4 recalls the pre-processing parameters.

The subdivision into ROI generates 1530 ROIs. Each ROI contains on average 80,000 points, representing the ground surfaces. Geometric and Local features are then computed for each ROI. Geometric features to be used in the following steps are computed with CloudCompare on the whole point cloud. Three *radii* for the neighbourhood selection used are, respectively 0.05, 0.08, and 0.10 m. From the geometric feature *Point density* it is possible to identify that the average point density on the ground is 5000 points for each square metre.

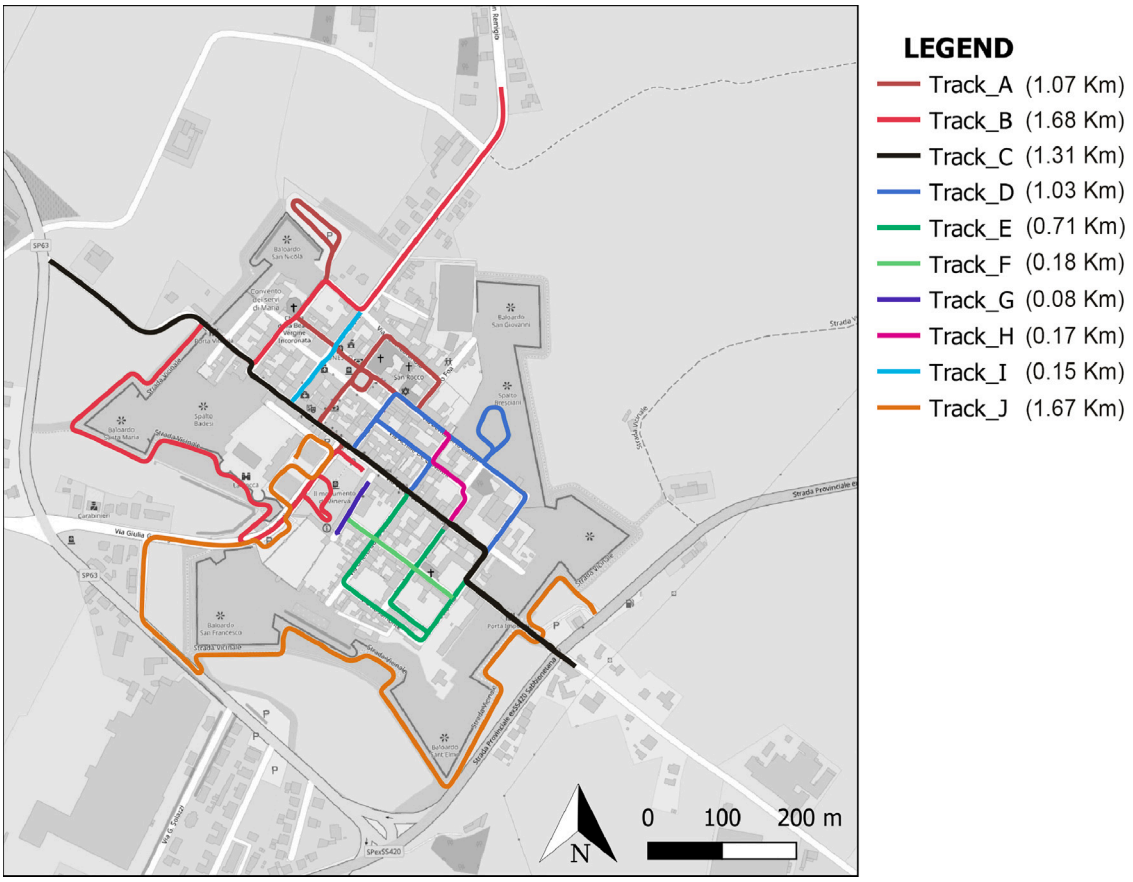

Fig. 13. Map of the city of Sabbioneta. The survey is conducted with a MLS system: Leica Pegasus:Two. The city is surveyed by 10 acquisition missions, reported on the legend on the right. Near each scan mission name, its length is reported in kilometres, the total length is almost 7 km. Acquisition track "C" (in black) is used as training dataset in both ML and DL approaches.

Table 5
Values of the paving material segmentation parameters used in the method.

Parameter	Value
Cell size	0.02 m
R-channel feature	Intensity
G-channel feature	Omnivariance (radius = 0.05 m)
B-channel feature	Roughness (radius = 0.05 m)
image re-size	500 × 500 pixels
DL classes	sampietrini, bricks, cobblestones, stones, asphalt, background

Table 6
Performance metrics for the DL classification of Sabbioneta dataset. They are computed on the point cloud after the classified images are reprojected back onto the ROI points.

Class	Precision	Recall	F1-score
background	0.99	0.98	0.99
sampietrini	0.92	0.97	0.94
bricks	0.93	0.82	0.87
cobblestones	0.93	0.98	0.95
stone	0.84	0.93	0.89
asphalt	0.86	0.94	0.90

4.2.2. Paving materials segmentation

For the DL classification, ROIs are rasterized, and cell size is set to 0.02 m. Pixel values for channels RGB are set as the average of three specific point features. After a visual inspection of the point cloud, the features selected are the ones considered the most representative of differences in pavings. The features are Intensity, stored in the R channel, Omnivariance, stored within the G channel, and Roughness, stored within the B channel. Features used were calculated with a neighbourhood radius of 0.05 m. For the purpose of DL classification, the image size is transformed to 500 × 500 pixels, and then after the classification, they are transformed back to the original size. Parameters are reported in Table 5.

DL classes are defined after an on-site inspection of pavings, made by experienced technicians. For Sabbioneta, the most representative and diffuse pavings, and so the classes, are *sampietrini, bricks, cobblestones, stones, aspalth*. These classes are depicted by Fig. 14. An extra class, *background*, is set for the pixels of the image which do not represent any point, required by the rasterization process. For the training dataset ROIs from Track C are selected, from the most representative road of the city, including all pavings.

The trained model is applied to all other ROIs to classify pavings; classified images are reprojected back onto points. Focusing on the point cloud and on the predicted paving material of each point, it is possible to compute the confusion matrix (Fig. 15), and the performance metrics (Table 6). The average accuracy of the prediction, computed as the ratio between the correctly classified points over the total, is 99.08%. Fig. 16 shows some rasterized ROIs and the predicted paving material by the DL workflow.

4.2.3. Ground elements segmentation

Parameters for the RF classifier are selected as follows. All the parameters for the `scikit-learn` library RF constructor were left to the default value. The feature selection is conducted by exploiting the Feature Importances plot (Fig. 17). All features, global and local, are included in the graph; geometric features computed using three *radii* for the neighbourhood selection are included. From this graph and after reasoning on the meaning of features, some of them are selected for the ML classification. For the geometric features, only the

Fig. 14. Classes of materials used for DL classification for Sabbioneta.

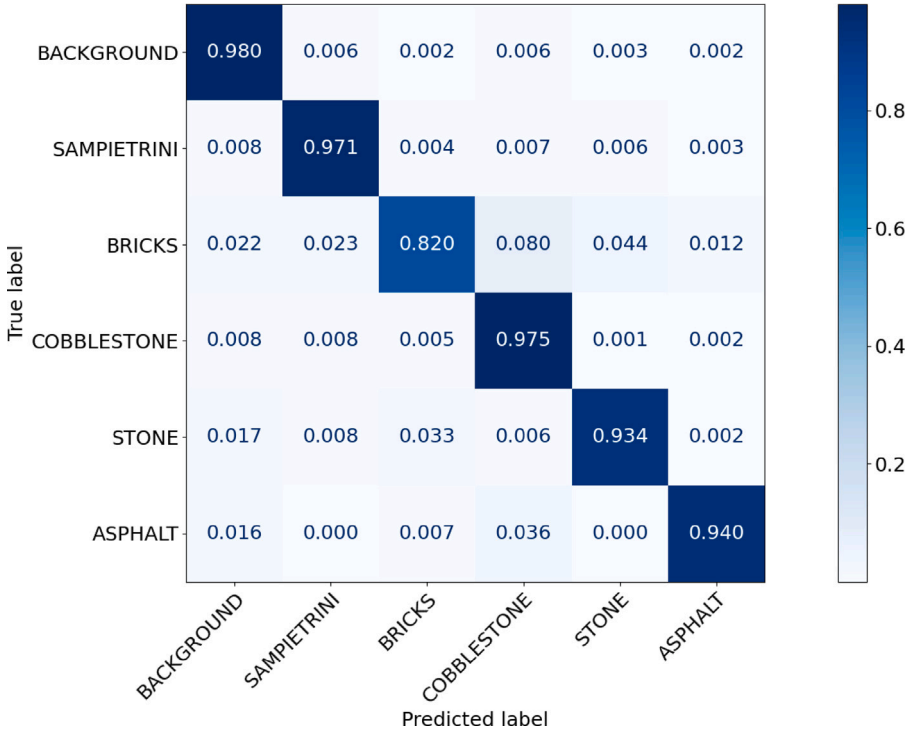

Fig. 15. Normalized by rows confusion matrix for paving material segmentation, classes are *background, sampietrini, bricks, cobblestone, stone, asphalt*.

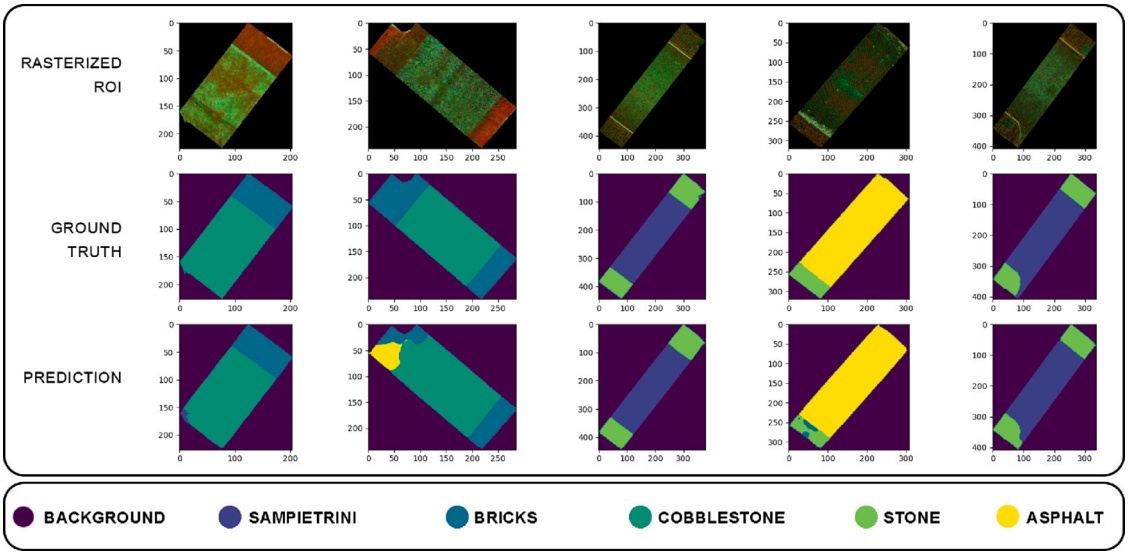

Fig. 16. Some of the rasterized ROIs from the case study. The correspondent Ground Truth, and the DL prediction are reported below each ROI. A legend is reported at the bottom of the image.

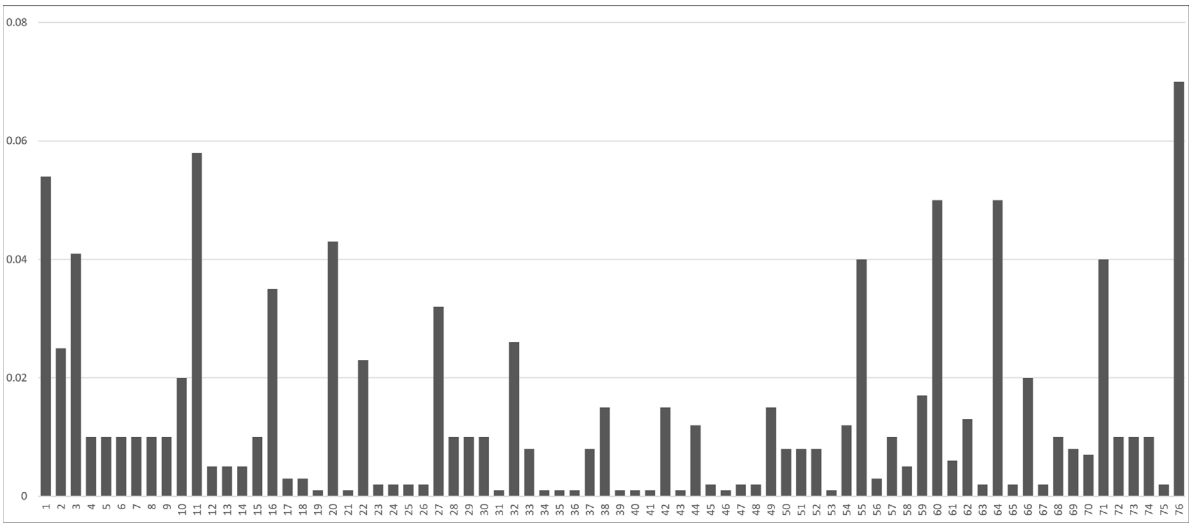

Fig. 17. Feature Importances plot computed for the ML classification. This plot is used to determine which features to use for the Random Forest classification and shows the importance of each feature for the ML process. On the *x*-axis the Features, and on the *y*-axis their importance value. In order to make the values on the *x*-axis more readable, numerical indices have been inserted in the graph, and the names of the corresponding features are given below. The geometric features are calculated with 3 different neighbourhood search radii (0.05, 0.08, 0.10 m).

Table 7
Values of the ground elements segmentation parameters used in the method.

Parameter	Value
Classes	road, sidewalk
RF classification features	Intensity, d-rel, Zrel, Roughness (0.1), Omnivariance (0.1), H, S, Z, Normal change rate (0.1), Anisotropy (0.1), Sphericity (0.1)

Table 8
Precision metrics for the ML classification of the Sabbioneta dataset.

Class	Precision	Recall	F1-score
sidewalk	0.89	0.81	0.85
road	0.82	0.90	0.86

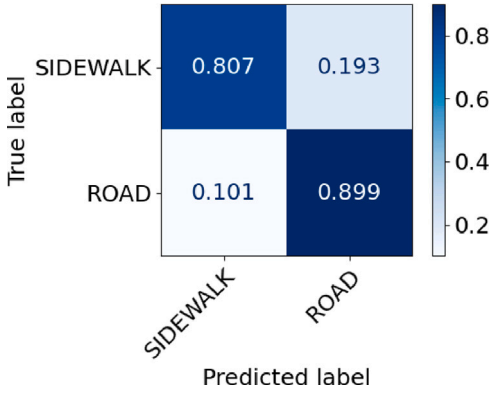

Fig. 18. Normalized by rows confusion matrix for ground elements segmentation, classes are *road* and *sidewalk*.

ones computed by a higher radius are selected. Selected features are presented by Table 7. Among the features chosen, there are global (geometric, radiometric) and local ones.

The training dataset is selected among the most representative ROIs from track C, the same used for DL segmentation. The trained model is then applied to segment all the other ROIs. Confusion matrix (Fig. 18) and precision metrics are computed (Table 8). The average accuracy, computed as the ratio between the correctly classified points over the total, is 88.2%. A top view of the classified Sabbioneta point cloud is shown in Fig. 19.

4.2.4. Sidewalks' attributes computation

The calculation of sidewalk attributes is done by following the equations shown in previous sections. Table 9 summarizes the average values of attributes. The resulting values are also compared with the legal minimums related to physical accessibility with reference to Italian laws (Ministerial Decree n. 236/89 and Decree of the President of the Republic n. 503/96).

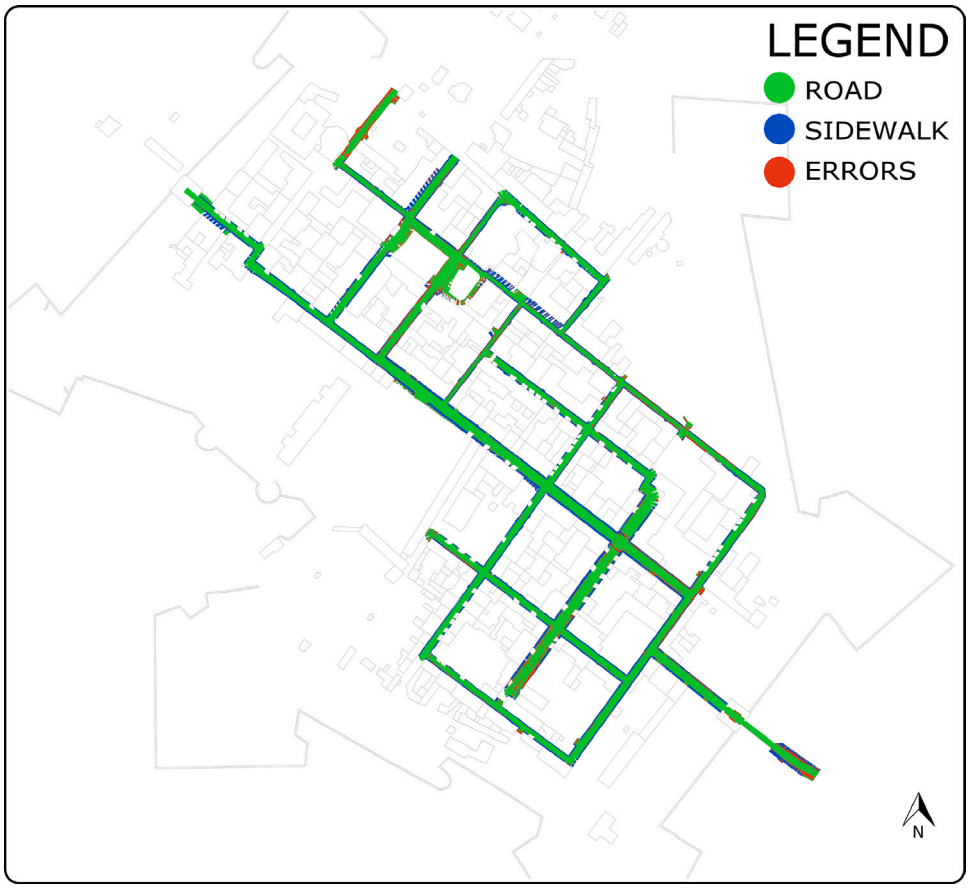

Fig. 19. Top view of the point cloud of Sabbioneta, superimposed to buildings polygons from OSM. The point cloud is coloured according to *sidewalk* and *road* segmentation. Misclassified points are depicted in red. (For interpretation of the references to colour in this figure legend, the reader is referred to the web version of this article.)

Table 9
Results of the Attributes computed for each sidewalk segment. For each attribute, the range of values is presented and compared with the Italian laws reference value (Ministerial Decree n. 236/89 and Decree of the President of the Republic n. 503/96). Also, the percentage of accessible segments out of the total is reported.

Attribute	Ranges	Most frequent	Reference value	Accessible segments
Width	0.45 m ÷ 2.20 m	0.95 m	≥ 0.90 m	72.3%
Transverse slope	0.05% ÷ 9.75%	1.25%	≤ 1%	8.6%
Longitudinal slope	0.10% ÷ 9.77%	2.1%	≤ 5%	79.3%
Relative Z difference	0 m ÷ 0.12 m	0 m	≤ 0.025 m	66.5%

4.2.5. Representation

In order to generate the vector file, it is necessary to first proceed with the identification of crossings. Specifically, 34 *L-shaped* crossings, 52 *T-shaped* crossings, and 10 *X-shaped* crossings are identified in the city of Sabbioneta.

The automatically generated vector file is composed of 1780 nodes and 1720 edges. Manual refinement is done for a few missing or erroneously generated edges. A total of 23 edges are refined, corresponding to 1.3% of the total.

In Sabbioneta there are only two zebra crosswalks; according to Italian regulation (Article 190 of the Highway Code), in urban or suburban roads, if there are no crosswalks or the closer zebra crossing is farther than 100 m, it is possible to cross the street without passing on the zebra crossing. In trying to mimic this scenario, additional edges are inserted into the network, so that in the route calculation the crossing of the street, at any point, can be provided. This second-level network is composed of 1357 extra edges (for a total of 3077 edges). Fig. 20 shows the vectorization process applied on Sabbioneta and a portion of the network with the two types of edges: regular ones (in blue), and the ones considering the possibility of crossing the street without using zebra crossing (in fuchsia). These last edges type connects edges on opposite sides of the road. They could be used for navigation purposes allowing the computed path to cross the street in every position.

The shapefile with sidewalk network is published on GitHub (github.com/HeSuTech), in order to make it easily available to all possible interested users. Furthermore, the shapefile is submitted to the Italian OSM community, which approved the file as suitable for the uploading on OSM database. The process has begun, carried out by the community itself, and can be followed on the special web page created on the OSM-wiki website (wiki.openstreetmap.org/wiki/Import/Catalogue/Sabbioneta_Sidewalk_Import).

The vector file is then used to compute paths within the city. Here we present one example, derived from Treccani et al. (2022b). The QGIS tool allows the computation of the shortest path between two points, but acting on the speed value of each edge it is possible to compute the fastest path. In order to compute an accessible path, for example selecting only sidewalks with accessible width (at least 0.9 m according to Italian law), a very low speed (0.001 km/h) is assigned to inaccessible edges, while a relatively higher speed is set to accessible edges (4 km/h). The result is a path that tends to be on accessible sidewalks (Fig. 21).

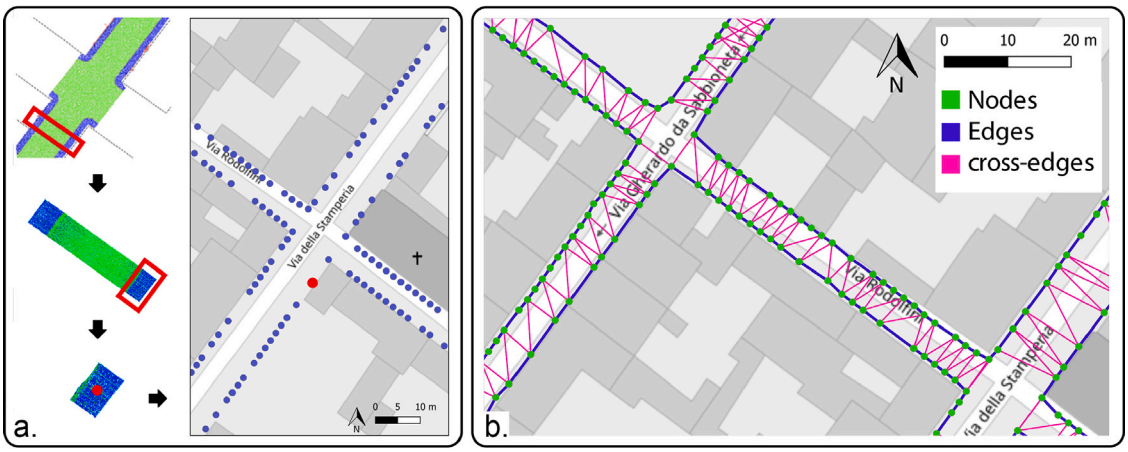

Fig. 20. Vectorization process in Sabbioneta. (a) Scheme of the vectorization for ROIs of Sabbioneta, where for each ROI the centre of the cluster of points segmented as *sidewalk* are transformed into nodes for the sidewalk vector network. (b) a portion of the sidewalk network, with two types of edges, the regular ones (in blu) connecting consecutive edges, and the cross-edges (in fuchsia) used to mimic the possibility of crossing the road everywhere in the absence of zebra crossing in the vicinity.
Source: Images modified from Treccani et al. (2022b).

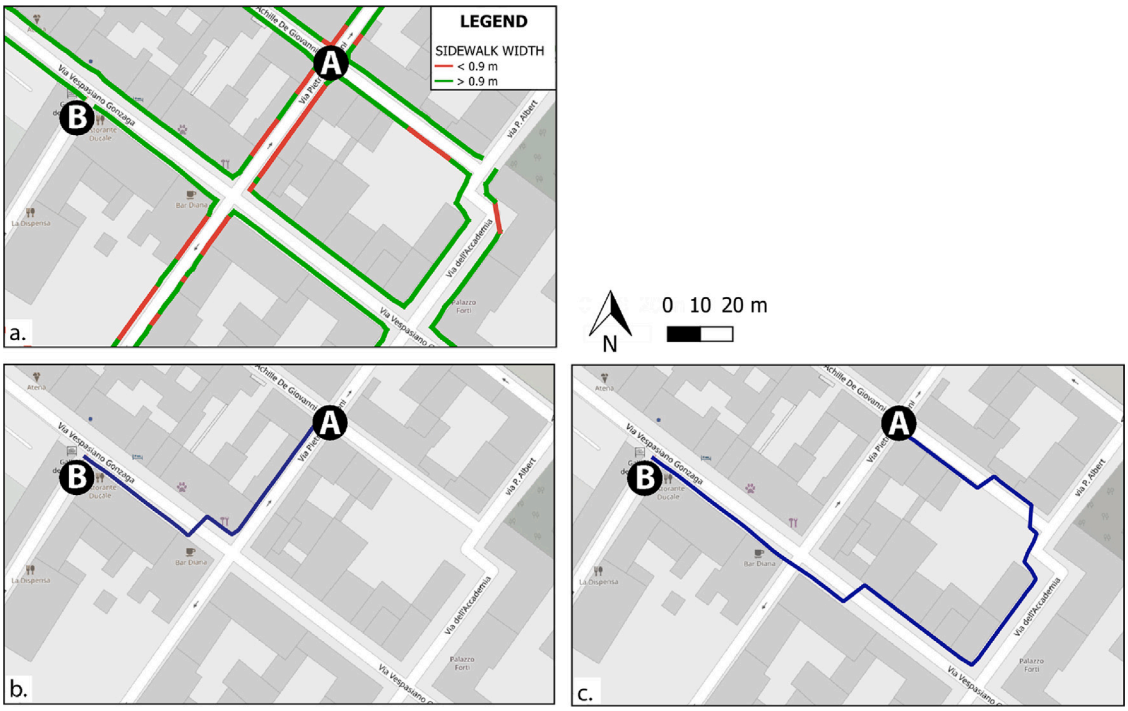

Fig. 21. Path computed on the basis of the generated shapefile. Two different paths are computed using the generated vector network and QGIS. (a) the generated sidewalk network of Sabbioneta, sidewalks edges are coloured according to their width, according to Italian law, the width is accessible if > 90 cm (coloured in green), otherwise the sidewalk is not accessible (in red). (b) Computed path to move from A to B considering the shortest path. (c) Computed path considering the width value as a weight, the result is the most accessible path according to Italian law for sidewalk widths. (For interpretation of the references to colour in this figure legend, the reader is referred to the web version of this article.)
Source: Images modified from Treccani et al. (2022b).

4.3. Discussion

The method presented and tested on Sabbioneta proves to be capable of analysing pedestrian mobility in historic urban environments. Although quite limited in size, the city has elements of interest and distinctive features, such as the use of different materials for paving, streets with different widths, and a large number of crossings and one-way streets. The use of this method on Sabbioneta proves its effectiveness in historical cities, and thus could be imagined its possibility of use in historical settings with similar scenarios.

During the preprocessing of the data, several features are computed, which proved to be crucial for subsequent stages. Although geometric features were calculated with different *radii*, those actually used by the ML and DL procedure are only a few and with specific *radii* (0.005 m for DL and 0.1 for ML). The choice of these features is the result of reasoning based on empirical tests and on the basis of statistical graphs made during the workflow. Among these features, the local ones (i.e., Z_{rel} and d_{rel}) proved to be of fundamental importance for the proper execution of the method.

ROIs were selected with a fixed width, of 2 m. This value allowed not only to reduce the memory consumption by the computer but mainly to obtain an output shapefile with sidewalk information with high resolution: data every 2 m along the sidewalk route. To properly select ROIs, the trajectory data is necessary. In case such data is

missing, it should be fictitiously generated, for example using road lines from OSM or using other specific methods suited to the purpose.

DL image segmentation approach is capable of correctly identifying the city's pavements. Analysing the performance metrics it is possible to note that improvements could be done for *bricks* and *stone* classes. It should also be noticed that *asphalt* paving is only in few areas of the city. In some areas of the city, the paving is so damaged that its roughness can lead to errors in segmentation. In such cases, damaged *stone* or damaged *sampietrini* are very similar to *cobblestone* paving. Anyway, it is important to note that in the method, the paving attribute is assigned as the most present on the sidewalk cluster of points analysed, so local segmentation errors can be avoided.

Important is the choice of cell size and the resolution during rasterization phase. This value should also be chosen accordingly to the density of points on the ground. Rasterized images should be such that they have uniformly distributed pixels, so there should be no missing data (background pixels) between other pixels.

Segmentation of the point cloud through RF classification is able to correctly segment ROIs into *sidewalk* and *road*. An important assumption is the presence of sidewalks; in fact, for the vast majority of the city, sidewalks are present on both sides of the street, so in cases where they are present only on one side, it happens that there are some false positives in the prediction. From the test made developing the method, the d_{rel} feature proved to be crucial for the ML segmentation.

Given the good results obtained with ML for *sidewalk* and *road* segmentation, we tested a similar ML-based approach to perform the task of paving materials segmentations. Since the results obtained with this approach showed very poor accuracy, we decided to perform the paving material segmentation task with a different approach. We decided to apply DL segmentation methods to the rasterized point clouds, which showed very high accuracy results. The choice of these two separated approaches was crucial for reaching higher accuracy results for both tasks, which are fundamental for the subsequent phases of the presented workflow.

Concerning attribute calculation, the information extracted from the sidewalks provides a large amount of data for analysing the sidewalks of the city. These attributes are very useful because they allow rapid identification of portions where to focus the attention for planned maintenance or to make improvements, allowing more thoughtful decisions.

The choice of the shapefile format is the result of balancing the desire to reach the largest number of end users with maintaining a rigorousness of the final data. In fact, even if point cloud representation techniques exist, it was considered that a vector file is easier to be understood and used by a wider range of final users independently of their experience in Geomatics.

Although not presented in this article, the vector file can be easily used to generate thematic maps, by showing different themes on the edges of the shapefile. In addition, by comparing attribute values with National regulations, edges can be coloured according to their compliance or noncompliance.

Lastly, the very accurate vector file generated allows the analysis and management of pedestrian mobility within the city. As an example, path calculation proved to be very easy to perform based on the vector file made. Although a specific open-source tool was used in this article, the great interoperability of the shapefile format makes the generated file usable by other software and in other procedures. In addition, the positive feedback from the Italian OSM community on the possibility of uploading the vector file to the OSM database makes it clear how effective and readily usable the output of the presented method is.

5. Conclusions

In this paper, a method for the automatic characterization of the navigable space for pedestrians in historic urban areas from point clouds is presented. The input point cloud dataset is analysed through ML and DL approaches, identifying paving materials and ground elements. Geometric attributes of sidewalks are then computed and conveyed into a network made available in vector format. The method is successfully tested on an Italian historic city: Sabbioneta.

The method aims to propose a complete strategy that, from an initial datum (point cloud), and through a series of automatic procedures, allows obtaining an output datum (a shapefile) that can be easily exploited for an accurate calculation of routes. Apart from the initial geometric features computation, which is done with CloudCompare, and the path computation, which is done with QGIS, the workflow for the production of the output shapefile is completely implemented through *Python* scripting.

The resulting sidewalk network data certainly provides a basis for various future developments, depending on the end user. For example, it can be used by technical experts, as a basis for making maintenance and urban design plans; it can be used by public administrations to make informed decisions and guide their policies; and it can be made available in a variety of ways to citizens and tourists, who can use its potential for planning their daily movements in the city.

The promising results obtained from this research allow foreseeing various future developments. The method will be tested on a larger scale, on cities of greater extents, and with source data obtained from a different instrument than the presented one, for example using terrestrial laser scanners (TLS), aerial laser scanners (ALS), or portable mobile mapping systems (PMMS). It is also planned to make more use of the output shapefile. Concretely, The possibility of making it usable on a web platform will be explored and a more refined method of calculating routes will be studied. Besides, the output shapefile will be combined with a city model to perform improved mobility analyses.

CRediT authorship contribution statement

D. Treccani: Conceptualization, Methodology, Investigation, Software, Visualization, Writing – original draft, Writing – review & editing. **A. Fernández:** Methodology, Software, Validation, Supervision. **L. Díaz-Vilariño:** Conceptualization, Methodology, Validation, Supervision, Writing – review & editing. **A. Adami:** Conceptualization, Resources, Validation, Supervision.

Declaration of competing interest

The authors declare that they have no known competing financial interests or personal relationships that could have appeared to influence the work reported in this paper.

Data availability

Data will be made available on request

Acknowledgements

Authors would like to thank Leica Geosystem Italy for providing the instrument Leica Pegasus:Two and technical support to raw data processing. This work was partially supported by human resources grant RYC2020-029193-I funded by MCIN/AEI/10.13039/501100011033 and FSE "El FSE invierte en tu futuro", by grant ED431F2022/08 funded by Xunta de Galicia, Spain-GAIN, and by the projects PID2019-105221RB-C43 funded by MCIN/AEI/10.13039/501100011033 and PCI2022-132943, funded by MCIN/AEI/10.13039/501100011033 and by the European Union "Next Generation EU"/PRTR. The statements made herein are solely the responsibility of the authors.

References

Ai, C., Tsai, Y.J., 2016. Automated sidewalk assessment method for Americans with disabilities act compliance using three-dimensional mobile lidar. Transp. Res. Rec. 2542 (1), 25–32. http://dx.doi.org/10.3141/2542-04.

Arenas, R., Arellano, B., Roca, J., 2016. City without barriers, ICT tools for the universal accessibility. Study cases in Barcelona. In: International Conference on Virtual City and Territory. "Back to the Sense of the City". Krakow, Poland.

Balado, J., Díaz-Vilariño, L., Arias, P., González-Jorge, H., 2018. Automatic classification of urban ground elements from mobile laser scanning data. Autom. Constr. 86 (September 2017), 226–239. http://dx.doi.org/10.1016/j.autcon.2017.09.004.

Balado, J., Díaz-Vilariño, L., Arias, P., Lorenzo, H., 2019. Point clouds for direct pedestrian pathfinding in urban environments. ISPRS J. Photogramm. Remote Sens. 148 (January), 184–196. http://dx.doi.org/10.1016/j.isprsjprs.2019.01.004.

Corso Sarmiento, J., Casals Fernández, J., 2017. Obtaining optimal routes from point cloud surveys. ACE-Archit. City Envron. 11 (33), http://dx.doi.org/10.5821/ace.11.33.5154.

European Commission, 2023. Smart cities. URL: https://commission.europa.eu/eu-regional-and-urban-development/topics/cities-and-urban-development/city-initiatives/smart-cities_en. (Accessed 10 January 2023).

Halabya, A., El-Rayes, K., 2020. Automated compliance assessment for sidewalks using machine learning. In: Construction Research Congress. pp. 288–295. http://dx.doi.org/10.1061/9780784482865.031.

Heidari, A., Navimipour, N.J., Unal, M., 2022. Applications of ML/DL in the management of smart cities and societies based on new trends in information technologies: A systematic literature review. Sustainable Cities Soc. 85, 104089. http://dx.doi.org/10.1016/j.scs.2022.104089.

Hosseini, M., Miranda, F., Lin, J., Silva, C.T., 2022a. CitySurfaces: City-scale semantic segmentation of sidewalk materials. Sustainable Cities Soc. 79, 103630. http://dx.doi.org/10.1016/j.scs.2021.103630.

Hosseini, M., Sevtsuk, A., Miranda, F., Jr., R., Silva, C., 2022b. Mapping the walk: A scalable computer vision approach for generating sidewalk network datasets from aerial imagery. SSRN Electron. J. http://dx.doi.org/10.2139/ssrn.4086624.

Hou, Q., Ai, C., 2020. A network-level sidewalk inventory method using mobile LiDAR and deep learning. Transp. Res. C 119 (December 2019), 1–14. http://dx.doi.org/10.1016/j.trc.2020.102772.

Ishikawa, K., Kubo, D., Amano, Y., 2018. Curb detection and accessibility evaluation from low-density mobile mapping point cloud data. Int. J. Autom. Technol. 12 (3), 376–385. http://dx.doi.org/10.20965/ijat.2018.p0376.

Kim, J., 2022. Smart city trends: A focus on 5 countries and 15 companies. Cities 123, 103551. http://dx.doi.org/10.1016/j.cities.2021.103551.

López-Pazos, G., Balado, J., Díaz-Vilariño, L., Arias, P., Scaioni, M., 2017. Pedestrian pathfinding in urban environments: Preliminary results. ISPRS Ann. Photogramm. Remote Sens. Spatial Inf. Sci. IV-5/W1, 35–41. http://dx.doi.org/10.5194/isprs-annals-IV-5-W1-35-2017.

Lorenzi, A., 2020. Sabbioneta. Progetto di una città. LetteraVentidue, Siracusa (in Italian).

Luaces, M.R., Fisteus, J.A., Sánchez-Fernández, L., Munoz-Organero, M., Balado, J., Díaz-Vilariño, L., Lorenzo, H., 2021. Accessible routes integrating data from multiple sources. ISPRS Int. J. Geo-Inf. 10 (1), http://dx.doi.org/10.3390/ijgi10010007.

Ma, L., Li, Y., Li, J., Wang, C., Wang, R., Chapman, M.A., 2018. Mobile laser scanned point-clouds for road object detection and extraction: A review. Remote Sens. 10 (10), 1–33. http://dx.doi.org/10.3390/rs10101531.

Marconcini, S., 2018. The urban scale of inclusion: Reflections and proposals for accessible public spaces. Igra Ustvarjalnosti - Creativity Game - Theory and practice of spatial planning 2018, 052–056. http://dx.doi.org/10.15292/IU-CG.2018.06.052-056.

Mobasheri, A., Deister, J., Dieterich, H., 2017. Wheelmap: the wheelchair accessibility crowdsourcing platform. Open Geosp. Data Softw. Stand. (ISSN: 2363-7501) 2 (1), 27. http://dx.doi.org/10.1186/s40965-017-0040-5.

Mortaheb, R., Jankowski, P., 2022. Smart city re-imagined: City planning and GeoAI in the age of big data. J. Urban Manag. http://dx.doi.org/10.1016/j.jum.2022.08.001.

Ning, H., Li, Z., Wang, C., Hodgson, M.E., Huang, X., Li, X., 2022. Converting street view images to land cover maps for metric mapping: A case study on sidewalk network extraction for the wheelchair users. Comput. Environ. Urban Syst. 95, 101808. http://dx.doi.org/10.1016/j.compenvurbsys.2022.101808.

Nys, G.A., Kharroubi, A., Poux, F., Billen, R., 2021. An extension of CityJSON to support point clouds. Int. Arch. Photogramm. Remote Sens. Spatial Inf. Sci. XLIII-B4-2021, 301–306. http://dx.doi.org/10.5194/isprs-archives-XLIII-B4-2021-301-2021.

Paz Mouriño, S.d., Balado, J., Arias, P., 2021. Multiview rasterization of street cross-sections acquired with mobile laser scanning for semantic segmentation with convolutional neural networks. In: IEEE EUROCON 2021 - 19th International Conference on Smart Technologies. pp. 35–39. http://dx.doi.org/10.1109/EUROCON52738.2021.9535645.

Pierdicca, R., Paolanti, M., Matrone, F., Martini, M., Morbidoni, C., Malinverni, E.S., Frontoni, E., Lingua, A.M., 2020. Point cloud semantic segmentation using a deep learning framework for cultural heritage. Remote Sens. 12 (6), http://dx.doi.org/10.3390/rs12061005.

Saha, M., Saugstad, M., Maddali, H.T., Zeng, A., Holland, R., Bower, S., Dash, A., Chen, S., Li, A., Hara, K., Froehlich, J., 2019. Project Sidewalk: A Web-Based Crowdsourcing Tool for Collecting Sidewalk Accessibility Data At Scale. Association for Computing Machinery, New York, NY, USA, ISBN: 9781450359702, pp. 1–14. http://dx.doi.org/10.1145/3290605.3300292.

Serna, A., Marcotegui, B., 2013. Urban accessibility diagnosis from mobile laser scanning data. ISPRS J. Photogramm. Remote Sens. 84, 23–32. http://dx.doi.org/10.1016/j.isprsjprs.2013.07.001.

Šurdonja, S., Giuffrè, T., Deluka-Tibljaš, A., 2020. Smart mobility solutions – necessary precondition for a well-functioning smart city. Transp. Res. Procedia 45, 604–611. http://dx.doi.org/10.1016/j.trpro.2020.03.051.

Treccani, D., 2022. Point Cloud Processing for Physical Accessibility Evaluation in Historical Urban Environments. The Case of UNESCO Site of Sabbioneta (Ph.D. thesis). Politecnico di Milano, URL: http://hdl.handle.net/10589/192194.

Treccani, D., Balado, J., Fernández, A., Adami, A., Díaz-Vilariño, L., 2022a. A deep learning approach for the recognition of urban ground pavements in historical sites. Int. Arch. Photogramm. Remote Sens. Spatial Inf. Sci. XLIII-B4-2022, 321–326. http://dx.doi.org/10.5194/isprs-archives-XLIII-B4-2022-321-2022.

Treccani, D., Díaz-Vilariño, L., Adami, A., 2022b. Accessible path finding for historic urban environments: feature extraction and vectorization from point clouds. Int. Arch. Photogramm. Remote Sens. Spatial Inf. Sci. XLVI-2/W1-2022, 497–504. http://dx.doi.org/10.5194/isprs-archives-XLVI-2-W1-2022-497-2022.

Wegen, O., Döllner, J., Richter, R., 2022. Concepts and challenges for 4D point clouds as a foundation of conscious, smart city systems. In: Gervasi, O., Murgante, B., Misra, S., Rocha, A., Garau, C. (Eds.), Computational Science and Its Applications – ICCSA 2022 Workshops. Springer International Publishing, Cham, pp. 589–605. http://dx.doi.org/10.1007/978-3-031-10536-4_39.

Weinmann, M., Jutzi, B., Hinz, S., Mallet, C., 2015. Semantic point cloud interpretation based on optimal neighborhoods, relevant features and efficient classifiers. ISPRS J. Photogramm. Remote Sens. 105, 286–304. http://dx.doi.org/10.1016/j.isprsjprs.2015.01.016.

Weinmann, M., Jutzi, B., Mallet, C., Weinmann, M., 2017. Geometric features and their relevance for 3D point cloud classification. ISPRS Ann. Photogramm. Remote Sens. Spatial Inf. Sci. IV-1/W1, 157–164. http://dx.doi.org/10.5194/isprs-annals-IV-1-W1-157-2017.

Yuan, L., Guo, J., Wang, Q., 2020. Automatic classification of common building materials from 3D terrestrial laser scan data. Autom. Constr. 110, http://dx.doi.org/10.1016/j.autcon.2019.103017.